ACCOUNTS
of chemical research

# Noble Metal Nanowires: From Plasmon Waveguides to Passive and Active Devices

SURBHI LAL,[‡] JASON H. HAFNER,[†,§] NAOMI J. HALAS,[*,†,‡,§]
STEPHAN LINK,[‡,§] AND PETER NORDLANDER[†,‡]

[†]*Department of Physics and Astronomy,* [‡]*Department of Electrical and Computer Engineering, and* [§]*Department of Chemistry, Laboratory for Nanophotonics, Rice University, Houston, Texas 77005, United States*

RECEIVED ON MAY 5, 2012

## CONSPECTUS

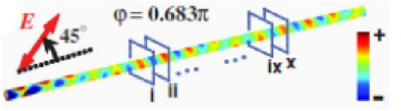


Using chemical synthesis, researchers can produce noble metal nanowires with highly regular, crystalline properties unachievable by alternative, top-down nanofabrication methods. Sitting at the intersection of nanochemistry and nanooptics, noble metal nanowires have generated intense and growing research interest. These nanostructures combine subwavelength transverse dimensions (50−100 nm) and longitudinal dimensions that can reach tens of micrometers or more, which makes them an ideal platform to launch surface plasmon waves by direct illumination of one end of the structure. Because of this property, researchers are using noble metal nanowires as a tool for fundamental studies of subwavelength plasmon-based optics and the properties of surface plasmon guided wave propagation in highly confined geometries below the classical optical diffraction limit. In this Account, we review some of the recent developments in plasmonic nanowire fabrication, nanowire plasmon imaging, and nanowire optical components and devices.

The addition of an adjacent nanowire, substrate, or other symmetry-breaking defect can enable the direct coupling of light to and from free space to the guided waves on a nanowire structure. Such structures lead to more complex nanowire-based geometries with multiple optical inputs and outputs. Additional nanowire imaging methods are also possible: plasmon propagation on nanowires produces intense near-field diffraction, which can induce fluorescence in nearby quantum dots or photobleach adjacent molecules. When the nanowire is deposited on a dielectric substrate, the plasmon propagation along chemically synthesized nanowires exceeds 10 $\mu$m, which makes these structures useful in nonlocal applications such as remote surface-enhanced Raman spectroscopy (SERS) sensing. Nanowires can be used as passive optical devices, which include, for example, polarization manipulators, linear polarization rotators, or even broadband linear-to-circular polarization converters, an optical function not yet achievable with conventional diffraction-limited optical components. Nanowires can also serve as highly directional broadband optical antennas.

When assembled into networks, plasmonic nanowires can be used to create optical devices, such as interferometric logic gates. Individual nanowires function as multiple input and output terminals in branched network geometries, where light incident on one wire can turn the emission from one or more output wires on or off. Nanowire-based devices that could exploit this effect include nanoscale routers and multiplexers, light modulators, and a complete set of Boolean logic functions.

## 1. Introduction

Noble metal nanostructures are a topic of intense current interest, with optical properties dominated by their collective electronic oscillations, known as surface plasmons. Much attention has been devoted to discrete noble metal nanoparticles and their assemblies, whose localized plasmon resonances provide a mesoscopic analogy with the molecular orbitals of simple quantum systems.[1] However, on extended metallic structures, surface plasmons propagate as charge-density waves at the metal surface. Chemically synthesized metallic nanowires with micrometer-scale lengths and nanoscale transverse dimensions support propagating surface plasmons with subwavelength lateral confinement. The modes of metallic wires in this size regime have been analyzed and studied extensively.[2,3] Here we examine plasmonic nanowires and their assemblies as practical building blocks for a remarkably broad range of subwavelength optical components.

## 2. Synthesis and Fabrication of Nanowires

Plasmonic waveguides are studied at visible and infrared frequencies with both chemically synthesized and

Published on the Web 10/26/2012 www.pubs.acs.org/accounts
10.1021/ar300133j 

lithographically fabricated nanowires. The nanowire diameters are subwavelength, but larger than 50 nm since very thin wires are expected to have low coupling efficiencies.[2] Due to smaller dissipative losses, propagation is more easily detected in Ag nanowires compared with Au, but both materials have been studied. Single-crystal nanowires made by chemical synthesis have been found to exhibit more facile propagation than polycrystalline nanowires produced by lithography.[4] Due to these factors, Ag nanowires synthesized by the polyol method[5,6] have been widely applied to studies of plasmon propagation. In this method, hot ethylene glycol or another polyol acts as both solvent and reducing agent. Silver nitrate is added, as well as the capping agent poly(vinyl pyrrolidone) and an agent to control oxidative etching. The reaction generally produces Ag nanowires >10 $\mu$m in length with 100−200 nm diameters and can be manipulated to produce nanowires with controlled lengths and diameters.[7]

Nanowire fabrication by electron beam lithography provides more control over waveguide geometry, allowing the design and manipulation of waveguide modes and their properties.[8] Plasmonic wedges and grooves have been studied, as well as tapered waveguides with spatially tunable resonances.[9] Further synthetic progress has also been made in the geometric control of chemically synthesized waveguides. We have recently shown that thin "nanobelts" with rectangular cross sections can be synthesized.[10] Gold nanobelts with 15−25 nm height, 25−100 nm width, and tens of micrometers in length are grown by the reduction of gold chloride in the presence of CTAB and SDS surfactants. Nanobelts have sufficiently small cross sections that their plasmon resonances are sharp as seen in dark field imaging (Figure 1). The observed nanobelt resonances are due to an asymmetric optical excitation across the nanobelt width and are tunable with cross sectional aspect ratio.[10] The nanobelt geometry is predicted to support a hierarchy of plasmon modes, an important property of interest for waveguides, devices, and complex optical networks.[10,11]

## 3. Imaging of Plasmon Propagation in Nanowires

Plasmons in nanowires are easily launched by illuminating one end of the structure with a tightly focused laser beam or an evanescent field created by total internal reflection.[4,12,13] Symmetry breaking at the nanowire ends enables the conversion between photons and plasmons, a process otherwise forbidden by momentum mismatch. Once launched, propagating plasmons are damped due primarily to absorption in the metal. For sufficiently long propagation distances, light is emitted at the distal nanowire end. However, since plasmons can also be reflected at the nanowire ends, the total light intensity detected at the end of a nanowire is not a reliable measure of the propagation distance. If the emitted intensity, $I_e$, is evaluated for many nanowires of different lengths, $L$, the $1/e$ damping $r$ can be obtained from[14]

$$I_e = I_0 C(d)\, e^{-L/r(D,d)}$$

where $I_0$ is the incident intensity, $C$ is the in-coupling efficiency, $D$ is the nanowire diameter, and $d$ is the thickness of a spacer layer separating nanowire and substrate. This approach allows us to investigate the influence of a substrate on nanowire plasmon damping. Figure 2a illustrates this measurement strategy for Ag nanowires with different $SiO_2$ spacer thicknesses on a Si substrate. As the $SiO_2$ thickness is decreased, the propagation distance becomes significantly shorter due to the coupling of plasmons to photonic modes of the substrate. This effect is even more pronounced for strongly absorbing substrates with larger dielectric permittivity.[7]

Even for nanowires of the same length, the average emitted intensity varies with substrate spacer thickness. In this example, the emission intensity (Figure 2b) reaches a

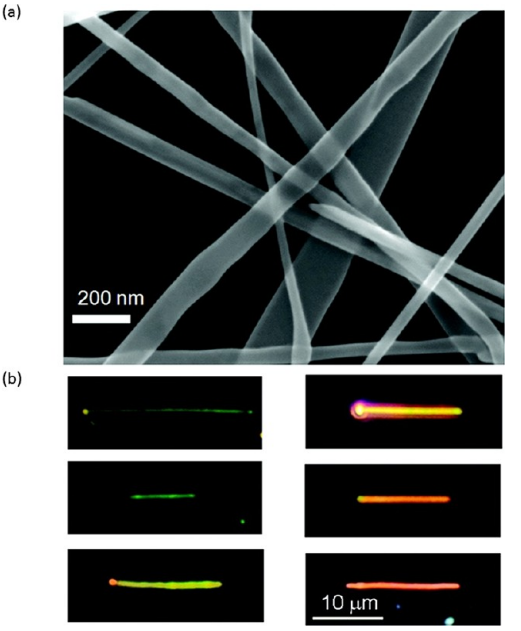


**FIGURE 1.** Gold nanobelts. (a) An SEM image of several nanobelts shows the range of widths. (b) Dark field images of several individual nanobelts show that the sharp plasmon resonances can be tuned through the visible wavelengths.[10]

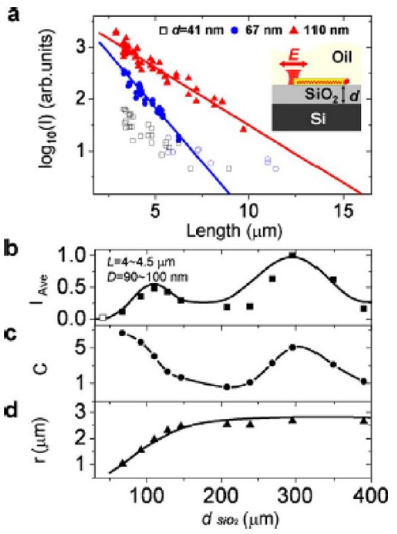


**FIGURE 2.** (a) Emission intensity from Ag NWs on layered substrates as a function of NW length, *L*. As illustrated in the inset, incident 633 nm light with polarization parallel to the NW is directed onto one NW end, while the light emitted from the other NW end is detected for various silica layer thicknesses, $d = 41$, 67, and 110 nm. When no light emission is observed, the scattered light at the NW end is recorded and represented by open symbols. (b) Average emission intensity for NWs of comparable length, $L = 4-4.5\ \mu$m, as a function of the silica layer thickness, *d*. The results from FDTD simulations are included as the curve. (c) In-coupling coefficient *C* and (d) $1/e$ damping length as a function of *d*.[14]

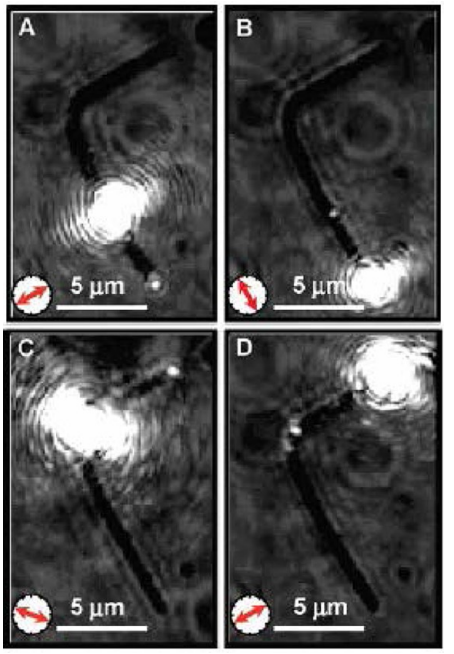


**FIGURE 3.** Bright field microscope images showing coupling between photons and NW plasmons at different points of broken symmetry. NW plasmons are excited by illumination (A) at the metallic nanoparticle adjacent to the NWs, (B) at the NW end, (C) at the NW kink, and (D) at the other NW end. The red arrows indicate the laser polarization that yielded maximum plasmon emission.[18]

maximum for $d \approx 110$ nm as a result of the competition between in-coupling efficiency (Figure 2c) and damping (Figure 2d). The variation in the in-coupling efficiency is caused by interference between incident and substrate-reflected light. Coupling efficiencies are also dependent on the geometry of the nanowire tip.[16] Because chemical synthesis produces nanowires with a variety of tip shapes and diameters, it is desirable to determine propagation distance along individual nanowires so that the effects of these parameters can be separated.

Monitoring the intensity of end emission can also be used to measure propagation distances along an individual nanowire for excitations at different locations along the structure. This is not possible with direct light excitation for a perfect nanowire. However, symmetry breaking introduced by a defect, such as a kink[17] or an adjacent nanoparticle, can serve as an antenna for the efficient in- and out-coupling of light.[13,18] Figure 3 shows optical images of a bent Ag nanowire with an adjacent nanoparticle, with the in-coupling of light at the nanoparticle (Figure 3A) and kink (Figure 3C), respectively.[18] Light emission from the end of the nanowire confirms the propagation of plasmons in both cases. Out-coupling of light at defects for end-excitation is also observed (Figure 3B,D). Using multiple input and output couplers one can determine the plasmon propagation distance along the nanowire.[13] Molecules,[19] quantum dots (QDs),[20] and dielectric waveguides[21] have also been employed to convert photons into plasmons through near-field excitation. One of the more flexible approaches for in-coupling is to use a tapered fiber that can be positioned precisely along the nanowire while the intensity of the end emission is monitored.[22,23]

If the spectrum of the end-emitted light is collected, both the propagation distance and the group velocity of the plasmon modes as a function of wavelength can be determined.[4,24−27] Key to this measurement is that part of the wave at the opposite nanowire end is reflected back into the nanowire, interfering with the incoming wave. This creates Fabry−Perot type resonances where the spacings between the maxima and minima in the measured spectrum yield the plasmon propagation distance and group velocity. However, care must be taken in the analysis, since interference between light emitted at the distal nanowire end can also interfere with the excitation beam, resulting in additional interference fringes.[26]

Although direct emission is often used to estimate the propogation distance in nanowires, it is not necessarily

reliable for reasons mentioned above, unless a large set of nanowires is studied. Direct imaging is therefore preferred. Imaging of the plasmon modes of nanowires can be achieved with subwavelength resolution using near-field scanning optical microscopy where the near-field is usually detected by a fiber scanned over the nanowire with optical excitation at one nanowire terminus.[4,28−30] Other nanowire imaging techniques include photoemission electron spectroscopy,[31] which detects emitted electrons after multiphoton excitation, electron energy loss spectroscopy,[32] and cathodoluminescence imaging,[33] where excitation is induced by an electron beam and the residual luminescence is detected.

Despite their lower resolution, optical far field methods have the advantage of being easier and less expensive to implement. To convert the plasmon into a free-space optical signal that can be detected in the far field, fluorescent molecules or semiconductor QDs can be placed on or adjacent to the nanowire: a spatially dependent fluorescent signal is excited through near field interactions with propagating plasmons.[26,34−38] Just as for absorbing substrates, fluorescent reporters constitute an absorbing superstrate and may similarly attenuate the propagating surface plasmon, affecting the accuracy of propagation length measurements. This method of fluorescence imaging is shown in Figure 4A for a single Ag nanowire.[37] The Ag nanowire is first coated with an $Al_2O_3$ spacer to avoid fluorescence quenching by the nanowire at close distances; then QDs are absorbed onto this layer. The bright field microscope image (i) shows the nanowire, while the fluorescence image recorded under wide-field illumination (ii) reveals a uniform coating of the QDs on the spacer layer. Fluorescence images recorded for excitation at the upper nanowire end as a function of laser polarization (iii−vi) provide a detailed image of plasmon propagation along the nanowire. These images reveal two important features: the fluorescence intensity decays exponentially along the NW, providing a direct measurement of propagation loss, and the field distribution shows a pronounced spatial modulation that depends upon input polarization. This modulation is due to the excitation and interference of multiple plasmon modes.[39] The specific amplitudes and phases of the modes are determined both by nanowire diameter and by polarization of the incident excitation beam. Because the near-field needs to be maximal for coupling from a nanowire to an adjacent nanostructure to occur, this spatial modulation controls the coupling of the nanowire plasmon to adjacent nanoparticles or nanostructures (Figure 4B).

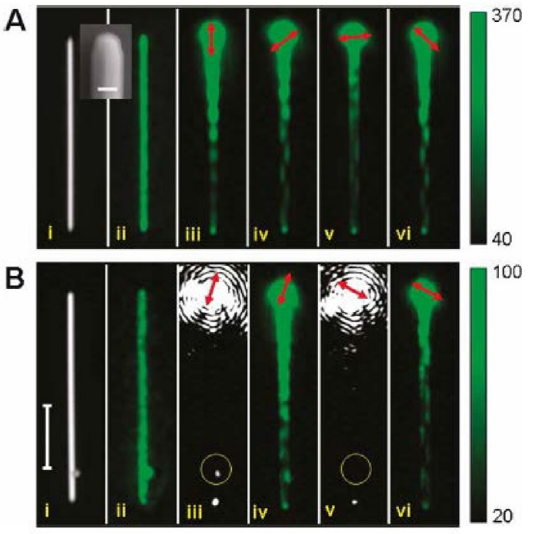


**FIGURE 4.** QD emission images of plasmons launched at one end of a Ag nanowire by 632.8 nm laser. Changing the laser polarization modifies the field distribution (A) and controls coupling to an adjacent Ag nanoparticle (B). (A) Optical (i) and SEM (inset) images of a Ag NW; (ii) QD emission image under wide-field excitation; (iii−vi) QD emission images as a function of incident polarizations. (B) Optical (i) and QD emission (ii) images of a NW with an adjacent NP system. Scattering (iii, v) and QD emission (iv, vi) images for two different polarizations. Scale bar = 200 nm (Ai); 5 $\mu$m (Bi), red arrows = laser polarization.[37]

In fluorescence-based imaging, it is generally difficult to obtain information regarding short propagation distances due to saturation of the fluorescence signal. However, by imaging the photobleached intensity of the fluorophore instead, this limitation can be overcome. This approach, called bleach-imaged plasmon propagation (BIIPP), is illustrated in Figure 5 for a Au nanowire excited at 532 nm, where the plasmons are strongly damped due to the Au interband transition.[40] Under low excitation powers, the fluorescence from molecules on top of the nanowire is recorded before (A) and after (B) coupling of the same excitation laser at higher excitation powers at the left end of the nanowire. The difference image (C) and corresponding line section of the photobeached intensity (D) enable one to determine the plasmon propagation length. The photobleached intensity caused by interaction with the propagating plasmons can be accumulated over long periods of time (tens of minutes), effectively amplifying the plasmon near-field relative to the laser excitation signal, a clear advantage of this approach (Figure 5E).

Another far-field microscopy technique that does not rely on the interaction between plasmons with nearby fluorophores is leakage radiation imaging.[17,41] For thicker nanowires (several hundred nanometers in diameter), plasmons

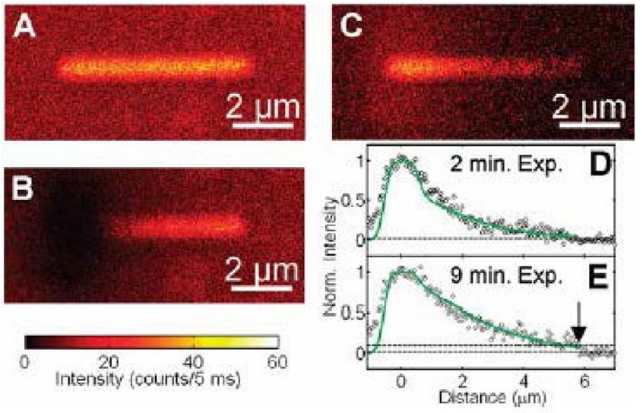


**FIGURE 5.** Bleach-imaged plasmon propagation (BIIPP). Fluorescence images recorded before (A) and after (B) continuous excitation of the left NW end for 9 min with a power of 40 nW. Difference image (C) and corresponding intensity line section taken along the long NW axis for a 2 min (D) and 9 min (E) exposure. The fits (green) yield a propagation distance of 1.7 $\mu$m. The arrow (E) marks the end of the NW where an offset in the photobleached intensity is visible due to accumulation of the photobleaching from the plasmonic near-field.[40]

decay radiatively and the radiation into the substrate can be imaged directly. Unlike the case of thin nanowires, where the output light is broadly divergent with minimal emission in the forward direction,[42] emission from thicker nanowires has been found to be remarkably unidirectional with an angular spread of only 4°.[43]

## 4. Nanowires as Passive Nanophotonic Devices

Ag nanowires support multiple plasmon modes. The presence of more than one mode excited along the nanowire is responsible for the spatial modulation along the length of the nanowire observed using quantum dot imaging (Figure 4). The lowest order modes and excitation conditions are illustrated in Figure 6. Here the angle $\theta$ denotes the angle of incident linear polarization with respect to the nanowire axis. The incident excitation is a paraxial Gaussian beam with an instantaneous electric field of the form $E_{inc} = E_0\, e^{-i\phi}$, where $\phi$ is the incident phase and $E_0$ is the mode profile of the incident light. For an input phase of $\phi = 0$, selective excitation of the $m = 0$ or $m = 1$ mode is achieved by aligning the incident polarization parallel ($\theta = 0°$) or perpendicular ($\theta = 90°$) to the wire axis. For an input phase of $\phi = \pi/2$, modes $m = -1$ or $m = 2$ modes are excited for $\theta = 0°$ or 90°, respectively.

For linearly polarized input light, a nanowire serves as either a polarization-maintaining waveguide or a polarization rotator (Figure 7).[16] The polarization change is found to depend sensitively on the geometrical shape of the

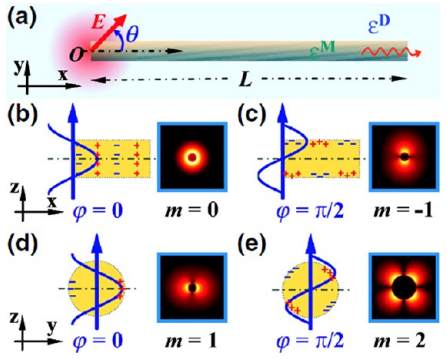


**FIGURE 6.** (a) Lowest order nanowire plasmons and excitation conditions. Excitation of the (b) $m = 0$ and (c) $m = -1$ modes at incident phases $\phi = 0$ and $\pi/2$ radians, for $\theta = 0°$ and of the (d) $m = 1$ and (e) $m = 2$ modes at $\phi = 0$ and $\pi/2$, for $\theta = 90°$. *E* field profile of each mode is shown in panels b–e.[38]

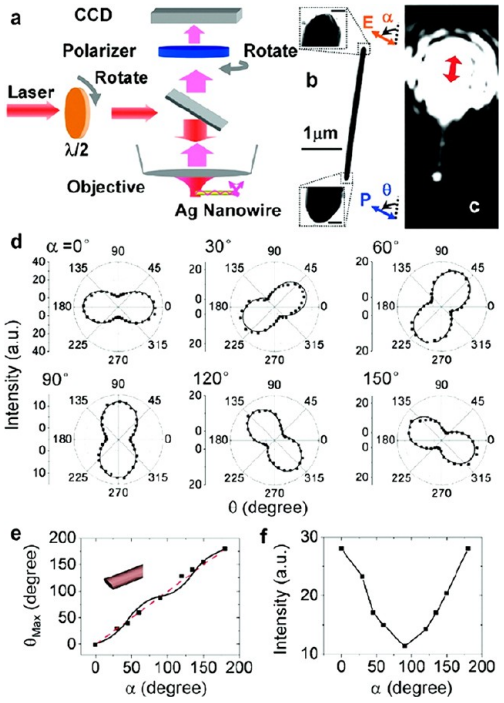


**FIGURE 7.** Polarization measurement. (a) Experimental schematic. (b) TEM image of 3.36 $\mu$m long nanowire with diameter of 130 nm. Scale bar = 50 nm. (c) Optical image of nanowire under 633 nm laser excitation. Red arrow: laser polarization. (d) Emission intensity as a function of polarization angle $\theta$, for 0°, 30°, 60°, 90°, 120°, and 150°. (e) Polarization of emission as a function of incident polarization. Dots, measured data; black curve, simulation result based on cylindrical wire with shape of both ends shown in inset. (f) Maximum emission intensity as a function of incident polarization angle.[16]

nanowire terminations. Theoretical analysis shows that the shape of the nanowire termination where the plasmon is launched determines the relative intensity of the SPP modes excited in the nanowire, which can modify the polarization of the emitted light. The shape of the emission end,

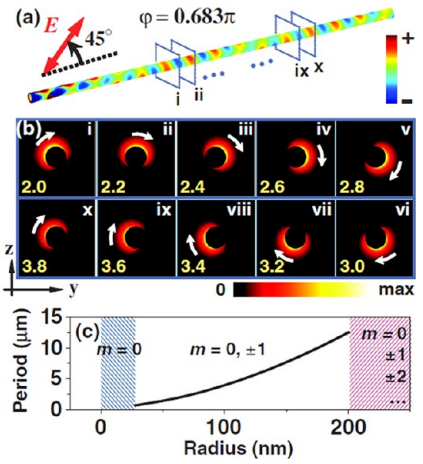


**FIGURE 8.** Chiral plasmons. (a) Surface charge density on a Ag nanowire. (b) Time-averaged power flow in the *yz*-plane at different positions along the nanowire, as indicated by the frames in panel a. (c) Period of the plasmon helix as a function of nanowire radius. Blue, single mode regime; magenta, multimode regime.[38]

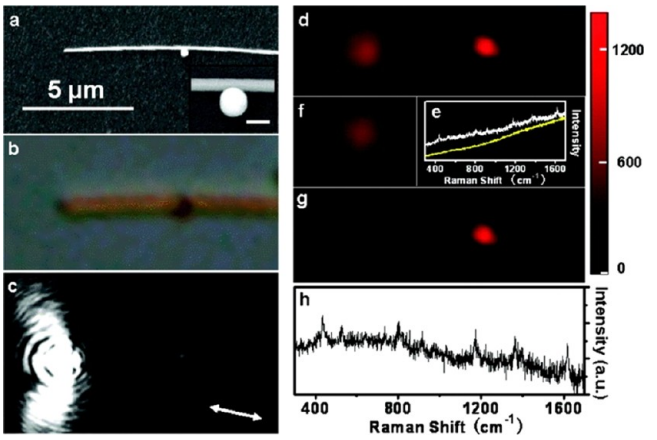


**FIGURE 9.** Remote SERS. (a) SEM image of nanowire−nanoparticle system. (b) Bright field optical image. (c) Optical image collected with a cooled CCD detector and 0.1 s integration time. (d) Raman image at the Stokes peak of 436 $cm^{-1}$. (e) Raman spectra from the laser spot at the left end (yellow) and remote wire/particle junction (white). (f) Fluorescence background image. (g) Raman image after background subtraction. (h) Remote-excitation SERS spectrum.[44]

on the other hand, influences both the spatial distribution and polarization of the emitted light.

For $\theta$ between 0° and 90°, the three lowest modes ($|m| \leq 1$) are excited simultaneously but with the $m = -1$ mode at a constant phase delay of $\pi/2$ with respect to the $m = 1$ mode. This phase delay enables a full range of elliptical SPPs to be generated along the nanowire. The coherent interference of two $m = \pm 1$ SPPs of equal amplitude results in a circularly polarized nanowire plasmon. The contribution of the simultaneously excited $m = 0$ mode is to stretch the circularly polarized SPP into a helical wave with a chiral near-field pattern. A typical charge distribution is shown in Figure 8a. The time-averaged power flow at various cross sectional positions of the nanowire (Figure 8b) shows how the electromagnetic energy revolves around the symmetry axis of the wire at the metal−dielectric interface as the SPP propagates along the structure. Figure 8c shows that chiral surface plasmons are excited only for a range of nanowire diameters: for narrower wires, only the lowest order nanowire SPP is excited; and for wider nanowires, multiple modes are excited simultaneously,[38] leading to a more complex multimodal structure and polarization behavior of the emitted light.

An interesting example of a nanowire-based optical component is a remote surface-enhanced Raman spectroscopy (SERS) sensor.[44,45] The optical "system" consists of a silver nanoparticle directly adjacent to a nanowire (Figure 9a). The nanoparticle−nanowire junction serves as the remote SERS output. When the nanowire end is illuminated, propagating SPPs induce a field enhancement in the remote nanoparticle−wire junction and result in a SERS signal from analytes present in that junction. In a simple, straightforward way, this result shows the potential for nanowire SPPs to propagate information in larger, more complex nanoscale optical systems.

## 5. Nanowires as Active Nanophotonic Devices

The properties of nanowire SPPs just discussed, when extended to systems of branched nanowires, result in active nano-optical devices such as routers, modulators, multiplexers, and logic gates.[46] In the branched nanowire system, plasmon propagation along the various branches is controlled by the amplitude and phase at the branch point. The plasmons propagating along one direction may also be redirected and modulated by applying a second laser input.

A branched nanowire excited at a single input but with a junction and two subsequent outputs serves as a plasmon router.[39] Here the plasmons launched along the main wire can also couple and propagate along the branched wire (Figure 10). The intensity of light emitted at either output depends strongly upon the polarization at the input nanowire terminus (Figure 10a). The nanowire plasmon can be switched[47] between outputs 2 and 3 by modifying the input polarization angle at 1. In Figure 10b,c, we see from the FEM simulations of this effect how the spatially modulated SPPs control this switching. In the case of a maximum evanescent field on the junction side of the branch point, a large fraction of the SPP energy propagates along the branch wire, transferred by tunneling of the evanescent wave. In the case

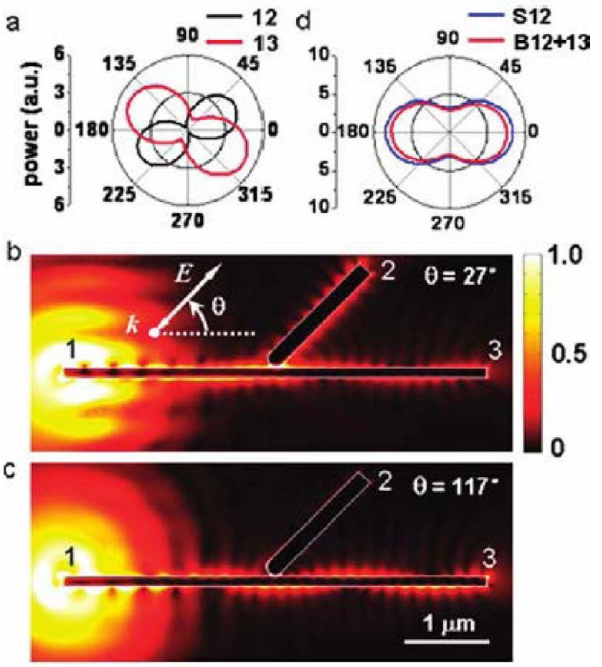


**FIGURE 10.** Plasmon router. (a) Calculated emission from terminals 3 (red) and 2 (black) as a function of incident polarization angle $\theta$ (indicated in panel b). (b,c) Local electric field distributions for maximal ($\theta = 27°$) (b) and minimal ($\theta = 117°$) (c) emission from the branch wire. (d) Emission power S12 (blue) from a single wire of same dimension as the main wire, compared with the total emission power B12 + 13 (red) from both terminals in the branched structure.[39]

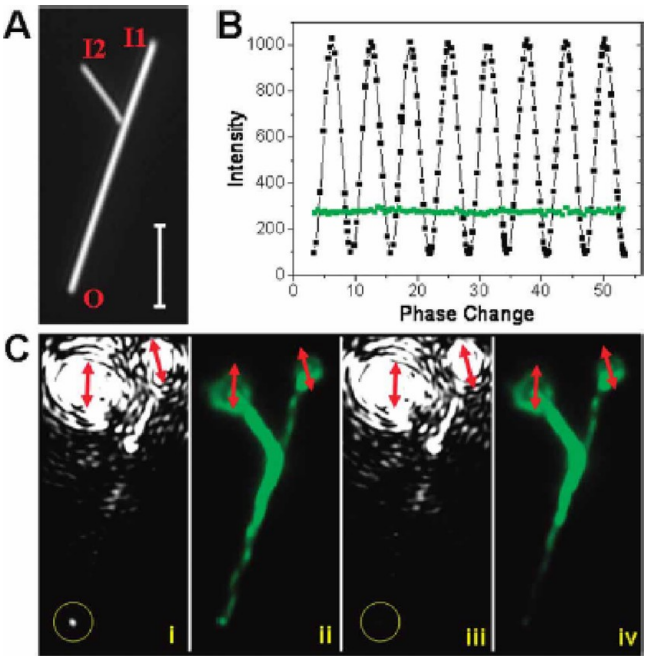


**FIGURE 11.** Interference of plasmons in Ag NWs. (A) Optical image of a two-nanowire network composed of a main nanowire and a secondary branch nanowire input. (B) Emission from O as a function of optical phase delay when input is either I1 or I2 (green); emission from O as a function of optical phase delay between I1 and I2 inputs (black). (C) (i, iii) Scattering images for phase shifted inputs I1 and I2. (ii, iv) QD emission images corresponding to i and iii. Red arrows indicate polarization of the input excitation laser.[37]

where the evanescent field is minimal at the branch point, the SPP continues to propagate on the main wire. Branched nanowires can also discriminate SPPs launched at distinct free space wavelengths and function as a multiplexer by independently switching and routing different wavelengths to different output branches.[39]

This branched nanowire routing behavior can also be exploited to design plasmon modulators. An example is Y-shaped branched nanowires consisting of a main wire and a short branch wire.[48] The short branch wire and the adjacent main wire ends serve as inputs I1 and I2, while the distal end of the main wire is the output O (Figure 11A). By changing the relative phase of the two incident laser beams, constructive/destructive interference of the plasmons propagating in the main wire occurs leading to a modulation of the emission from the output end (Figure 11B). At constant polarization, by change of the phase difference, a modulation depth of $I_{max}/I_{min} = 18$ can be achieved.[48] Similarly, by excitation of the two inputs with laser beams with zero phase difference but variation of the polarization of the input of the short branch wire, the plasmon propagating in the main wire can be modulated. The polarization dependent modulation can be understood in terms of the coupling efficiency of the branch wire plasmon to the main wire, and the subsequent constructive/destructive interference that occurs in the main wire.

The router and modulator concepts can be combined in branched nanowires with multiple inputs and outputs to realize a complete set of plasmonic logic circuits.[37] Plasmons propagating along branched Y-shaped nanowires, imaged using the QD imaging method described earlier, are shown in Figure 11. Plasmon logic can be illustrated as follows: if an excitation laser is incident at either I1 or I2, the output at O is constant. If both inputs are excited, the output intensity becomes dependent upon the relative phase or polarization of the two input fields and can be varied between a maximum and a minimum value (Figure 11B,C). With this large dynamic range, the intensities can be assigned ON and OFF states. By choice of relative phase and input polarization, this Y shaped branched NW can function as a XOR or OR logic circuit.[37] Similarly, a main wire with two branches, where one end of the main wire and an adjacent branch wire serve as inputs I1 and I2 and the far end of the main wire with an adjacent branch wire serve as output end O1 and O2, can be

**TABLE 1.** Schematic of Optical Logic Operations Possible on Nanowire Networks[a]

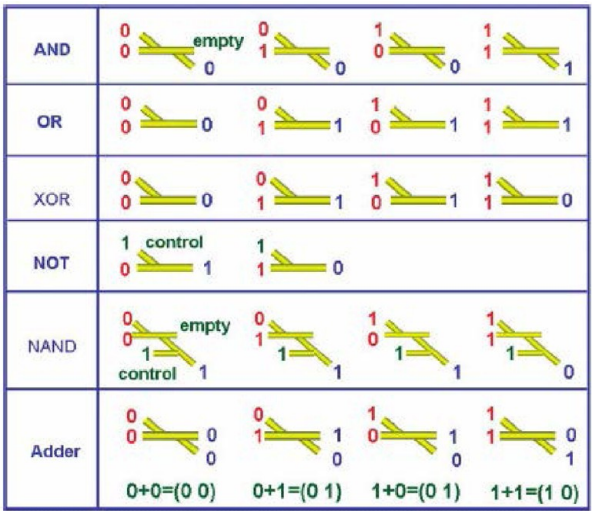


[a]The numbers in red are inputs, and those in blue are outputs. Unused terminals are labeled empty. The terminals labeled control require the input to be ON.[37]

designed to behave as an adder or AND gate. Table 1 shows a schematic depiction of logic circuits that can be designed using branched nanowires. More complex logic functions such as the NAND and NOR gates can also be realized using branched nanowires with two or more branches.[49]

## 6. Future Outlook

We have shown that chemically synthesized plasmonic metal nanowires are of significant interest and potential as nanoscale optical elements. As plasmon waveguides, we have begun to understand their propagation properties and coupling to adjacent plasmonic and excitonic structures. By positioning individual nanowires into multibranched structures, we have begun to realize passive and active nanooptical device functionalities. By further connecting and cascading structures into extended networks, more complex functions could be realized. This topical area is in its infancy but clearly has tremendous potential for optical frequency signal and information processing. However, much remains to be done. Nanowire-based logic gates do satisfy an important requirement of interferometric logic, the ability to maintain precise phase relationships between input arms of a device, that is extremely difficult to fulfill in a straightforward manner by other optical approaches. However, many practical requirements for applications, such as gain, fan-out, logic-level reset, and input–output isolation, have yet to be addressed. Recently, several promising strategies for implementing gain for propagating plasmons have been demonstrated.[50−53] The development of compatible electronic or nano-optical plasmon excitation and detection methods is also very important for future applications. As nanowire-based plasmon optics is developed, we can anticipate further advances addressing these challenges.

*This work was funded by the Robert A. Welch Foundation (Grants C-1220, C-1222, and C-1664). Link acknowledges support from NSF (Grant CHE-0955286). Lal, N.J.H., and P.N. acknowledge support from NSSEFF (Grant N00244-09-1-0067).*

BIOGRAPHICAL INFORMATION

**Surbhi Lal** is a research scientist in the Department of Electrical and Computer Engineering at Rice University. She received her Ph.D. from Rice University (2006) with Dr. Naomi Halas. Her research interests are fundamental nanophotonics and applications.

**Jason Hafner** is an Associate Professor at Rice University in the Department of Physics & Astronomy and Chemistry. His group studies plasmon resonances in gold nanoparticles and their biological and biomedical applications. His research interests also include electrostatic analysis of lipid membranes by atomic force microscopy. He is an Associate Editor of *ACS Nano*.

**Naomi Halas** is the Stanley C. Moore Professor of Electrical and Computer Engineering at Rice University. She pursues studies of light–nanoparticle interactions that give rise to new properties and effects, leading to applications in biomedicine, chemical sensing, and energy. She is a Member of the American Academy of Arts and Sciences and a Fellow of SPIE, APS, OSA, IEEE, and AAAS. She is an Associate Editor of *Nano Letters*.

**Stephan Link** is an assistant professor in the Departments of Chemistry and Electrical and Computer Engineering at Rice University. He received his Ph.D. from Georgia Tech (2000) with Mostafa El-Sayed and performed postdoctoral research with Paul Barbara (UT). The main interest of his research group is the study of the optical properties of plasmonic nanomaterials.

**Peter Nordlander** is a Professor of Physics and Astronomy and Electrical and Computer Engineering at Rice University. His group focuses on theoretical modeling of the optical and electronic properties of metallic nanostructures. He is a Fellow of APS, AAAS, and SPIE and an Associate Editor of *ACS Nano*.

FOOTNOTES

The authors declare no competing financial interest.

REFERENCES

1 Prodan, E.; Radloff, C.; Halas, N. J.; Nordlander, P. A hybridization model for the plasmon response of complex nanostructures. *Science* **2003**, *302*, 419–422.

2 Chang, D. E.; Sorensen, A. S.; Hemmer, P. R.; Lukin, M. D. Strong coupling of single emitters to surface plasmons. *Phys. Rev. B* **2007**, *76*, No. 035420.

3 Zia, R.; Schuller, J. A.; Brongersma, M. L. Near-field characterization of guided polariton propagation and cutoff in surface plasmon waveguides. *Phys. Rev. B* **2006**, *74*, No. 165415.

4 Ditlbacher, H.; Hohenau, A.; Wagner, D.; Kreibig, U.; Rogers, M.; Hofer, F.; Aussenegg, F. R.; Krenn, J. R. Silver Nanowires as Surface Plasmon Resonators. *Phys. Rev. Lett.* **2005**, *95*, No. 257403.

5 Sun, Y. G.; Xia, Y. N. Large-scale synthesis of uniform silver nanowires through a soft, self-seeding, polyol process. *Adv. Mater.* **2002**, *14*, 833–837.

6 Rycenga, M.; Cobley, C. M.; Zeng, J.; Li, W. Y.; Moran, C. H.; Zhang, Q.; Qin, D.; Xia, Y. N. Controlling the synthesis and assembly of silver nanostructures for plasmonic applications. *Chem. Rev.* **2011**, *111*, 3669–3712.

7 Coskun, S.; Aksoy, B.; Unalan, H. E. Polyol synthesis of silver nanowires: An extensive parametric study. *Cryst. Growth Des.* **2011**, *11*, 4963–4969.

8 Gramotnev, D. K.; Bozhevolnyi, S. I. Plasmonics beyond the diffraction limit. *Nat. Photonics* **2010**, *4*, 83–91.

9 Schnell, M.; Alonso-Gonzalez, P.; Arzubiaga, L.; Casanova, F.; Hueso, L. E.; Chuvilin, A.; Hillenbrand, R. Nanofocusing of mid-infrared energy with tapered transmission lines. *Nat. Photonics* **2011**, *5*, 283–287.

10 Anderson, L. J. E.; Payne, C. M.; Zhen, Y.-R.; Nordlander, P.; Hafner, J. H. A tunable plasmon resonance in gold nanobelts. *Nano Lett.* **2011**, *11*, 5034–5037.

11 Zhao, N.; Wei, Y.; Sun, N. J.; Chen, Q. J.; Bai, J. W.; Zhou, L. P.; Qin, Y.; Li, M. X.; Qi, L. M. Controlled synthesis of gold nanobelts and nanocombs in aqueous mixed surfactant solutions. *Langmuir* **2008**, *24*, 991–998.

12 Dickson, R. M.; Lyon, L. A. Unidirectional Plasmon Propagation in Metallic Nanowires. *J. Phys. Chem. B* **2000**, *104*, 6095–6098.

13 Sanders, A. W.; Routenberg, D. A.; Wiley, B. J.; Xia, Y. N.; Dufresne, E. R.; Reed, M. A. Observation of plasmon propagation, redirection, and fan-out in silver nanowires. *Nano Lett.* **2006**, *6*, 1822–1826.

14 Li, Z. P.; Bao, K.; Fang, Y. R.; Guan, Z. Q.; Halas, N. J.; Nordlander, P.; Xu, H. X. Effect of a proximal substrate on plasmon propagation in silver nanowires. *Phys. Rev. B* **2010**, *82*, No. 241402.

15 Aubry, A.; Lei, D. Y.; Maier, S. A.; Pendry, J. B. Plasmon hybridization between nanowires and a metallic surface: A transformation optics approach. *ACS Nano* **2011**, *5*, 3293–3308.

16 Li, Z. P.; Bao, K.; Fang, Y. R.; Huang, Y. Z.; Nordlander, P.; Xu, H. X. Correlation between incident and emission polarization in nanowire surface plasmon waveguides. *Nano Lett.* **2010**, *10*, 1831–1835.

17 Song, M.; Bouhelier, A.; Bramant, P.; Sharma, J.; Dujardin, E.; Zhang, D.; Colas-des-Francs, G. Imaging symmetry-selected corner plasmon modes in penta-twinned crystalline Ag nanowires. *ACS Nano* **2011**, *5*, 5874–5880.

18 Knight, M. W.; Grady, N. K.; Bardhan, R.; Hao, F.; Nordlander, P.; Halas, N. J. Nanoparticle-mediated coupling of light into a nanowire. *Nano Lett.* **2007**, *7*, 2346–2350.

19 Shegai, T.; Huang, Y.; Xu, H. X.; Kall, M. Coloring fluorescence emission with silver nanowires. *Appl. Phys. Lett.* **2010**, *96*, No. 103114.

20 Fedutik, Y.; Temnov, V. V.; Schops, O.; Woggon, U.; Artemyev, M. V. Exciton-plasmon-photon conversion in plasmonic nanostructures. *Phys. Rev. Lett.* **2007**, *99*, No. 136802.

21 Yan, R. X.; Pausauskie, P.; Huang, J. X.; Yang, P. D. Direct photonic-plasmonic coupling and routing in single nanowires. *Proc. Natl. Acad. Sci. U.S.A.* **2009**, *106*, 21045–21050.

22 Ma, Y. G.; Li, X. Y.; Yu, H. K.; Tong, L. M.; Gu, Y.; Gong, Q. H. Direct measurement of propagation losses in silver nanowires. *Opt. Lett.* **2010**, *35*, 1160–1162.

23 Wang, W. H.; Yang, Q.; Fan, F. R.; Xu, H. X.; Wang, Z. L. Light propagation in curved silver nanowire plasmonic waveguides. *Nano Lett.* **2011**, *11*, 1603–1608.

24 Allione, M.; Temnov, V. V.; Fedutik, Y.; Woggon, U.; Artemyev, M. V. Surface plasmon mediated interference phenomena in low-Q silver nanowire cavities. *Nano Lett.* **2008**, *8*, 31–35.

25 Kusar, P.; Gruber, C.; Hohenau, A.; Krenn, J. R. Measurement and reduction of damping in plasmonic nanowires. *Nano Lett.* **2012**, *12*, 661–665.

26 Wild, B.; Cao, L.; Sun, Y.; Khanal, B. P.; Zubarev, E. R.; Gray, S. K.; Scherer, N. F.; Pelton, M. Propagation lengths and group velocities of plasmons in chemically synthesized gold and silver nanowires. *ACS Nano* **2012**, *6*, 472–482.

27 Wiley, B. J.; Lipomi, D. J.; Bao, J. M.; Capasso, F.; Whitesides, G. M. Fabrication of surface plasmon resonators by nanoskiving single-crystalline gold microplates. *Nano Lett.* **2008**, *8*, 3023–3028.

28 Dorfmuller, J.; Vogelgesang, R.; Weitz, R. T.; Rockstuhl, C.; Etrich, C.; Pertsch, T.; Lederer, F.; Kern, K. Fabry-Perot resonances in one-dimensional plasmonic nanostructures. *Nano Lett.* **2009**, *9*, 2372–2377.

29 Krenn, J. R.; Lamprecht, B.; Ditlbacher, H.; Schider, G.; Salerno, M.; Leitner, A.; Aussenegg, F. R. Non-diffraction-limited light transport in gold nanowires. *Europhys. Lett.* **2002**, *60*, 663–669.

30 Verhagen, E.; Spasenovic, M.; Polman, A.; Kuipers, L. Nanowire plasmon excitation by adiabatic mode transformation. *Phys. Rev. Lett.* **2009**, *102*, No. 203904.

31 Douillard, L.; Charra, F.; Korczak, Z.; Bachelot, R.; Kostcheev, S.; Lerondel, G.; Adam, P. M.; Royer, P. Short range plasmon resonators probed by photoemission electron microscopy. *Nano Lett.* **2008**, *8*, 935–940.

32 Alber, I.; Sigle, W.; Muller, S.; Neumann, R.; Picht, O.; Rauber, M.; Aken, P. A. V.; Toimil-Molares, M. E. Visualization of multipolar longitudinal and transversal surface plasmon modes in nanowire dimers. *ACS Nano* **2011**, *5*, 9845–9853.

33 Vesseur, E. J. R.; de Waele, R.; Kuttge, M.; Polman, A. Direct observation of plasmonic modes in Au nanowires using high-resolution cathodoluminescence spectroscopy. *Nano Lett.* **2007**, *7*, 2843–2846.

34 Ditlbacher, H.; Krenn, J. R.; Felidj, N.; Lamprecht, B.; Schider, G.; Salerno, M.; Leitner, A.; Aussenegg, F. R. Fluorescence imaging of surface plasmon fields. *Appl. Phys. Lett.* **2002**, *80*, 404–406.

35 Graff, A.; Wagner, D.; Ditlbacher, H.; Kreibig, U. Silver nanowires. *Eur. Phys. J. D* **2005**, *34*, 263–269.

36 Verhagen, E.; Tchebotareva, A. L.; Polman, A. Erbium luminescence imaging of infrared surface plasmon polaritons. *Appl. Phys. Lett.* **2006**, *88*, No. 121121.

37 Wei, H.; Li, Z. P.; Tian, X. R.; Wang, Z. X.; Cong, F. Z.; Liu, N.; Zhang, S. P.; Nordlander, P.; Halas, N. J.; Xu, H. X. Quantum dot-based local field imaging reveals plasmon-based interferometric logic in silver nanowire networks. *Nano Lett.* **2011**, *11*, 471–475.

38 Zhang, S.; Wei, H.; Bao, K.; Hakanson, U.; Halas, N. J.; Nordlander, P.; Xu, H. Chiral surface plasmon polaritons on metallic nanowires. *Phys. Rev. Lett.* **2011**, *107*, No. 096801.

39 Fang, Y. R.; Li, Z. P.; Huang, Y. Z.; Zhang, S. P.; Nordlander, P.; Halas, N. J.; Xu, H. X. Branched silver nanowires as controllable plasmon routers. *Nano Lett.* **2010**, *10*, 1950–1954.

40 Solis, D.; Chang, W.-S.; Khanal, B. P.; Bao, K.; Nordlander, P.; Zubarev, E. R.; Link, S. Bleach-imaged plasmon propagation (BlIPP) in single gold nanowires. *Nano Lett.* **2010**, *10*, 3482–3485.

41 Bouhelier, A.; Wiederrecht, G. P. Surface plasmon rainbow jets. *Opt. Lett.* **2005**, *30*, 884–886.

42 Li, Z. P.; Hao, F.; Huang, Y. Z.; Fang, Y. R.; Nordlander, P.; Xu, H. X. Directional light emission from propagating surface plasmons of silver nanowires. *Nano Lett.* **2009**, *9*, 4383–4386.

43 Shegai, T.; Miljkovic, V. D.; Bao, K.; Xu, H. X.; Nordlander, P.; Johansson, P.; Kall, M. Unidirectional broadband light emission from supported plasmonic nanowires. *Nano Lett.* **2011**, *11*, 706–711.

44 Fang, Y. R.; Wei, H.; Hao, F.; Nordlander, P.; Xu, H. X. Remote-excitation surface-enhanced raman scattering using propagating Ag nanowire plasmons. *Nano Lett.* **2009**, *9*, 2049–2053.

45 Huang, Y. Z.; Fang, Y. R.; Sun, M. T. Remote excitation of surface-enhanced Raman scattering on single Au nanowire with quasi-spherical termini. *J. Phys. Chem. C* **2011**, *115*, 3558–3561.

46 Garnett, E. C.; Cai, W.; Cha, J. J.; Mahmood, F.; Connor, S. T.; Greyson Chrostoforo, M.; Cai, Y.; McGehee, M. D.; Brongersma, M. L. Self-limited plasmonic welding of silver nanowire junctions. *Nat. Mater.* **2012**, *11*, 241–249.

47 Cheng, M. T. Electric-field controlling a single plasmon transport in a metal nanowire. *Opt. Commun.* **2012**, *285*, 804–807.

48 Li, Z. P.; Zhang, S. P.; Halas, N. J.; Nordlander, P.; Xu, H. X. Coherent modulation of propagating plasmons in silver-nanowire-based structures. *Small* **2011**, *7*, 593–596.

49 Wei, H.; Wang, Z.; Tian, X.; Käll, M.; Xu, H. Cascaded logic gates in nanophotonic plasmon networks. *Nat. Commun.* **2011**, *2*, 387.

50 De Leon, I.; Berini, P. Amplification of long-range surface plasmons by a dipolar gain medium. *Nat. Photonics* **2010**, *4*, 382–387.

51 Noginov, M. A.; Podolskiy, V. A.; Zhu, G.; Mayy, M.; Bahoura, M.; Adegoke, J. A.; Ritzo, B. A.; Reynolds, K. Compensation of loss in propagating surface plasmon polariton by gain in adjacent dielectric medium. *Opt. Exp.* **2008**, *16*, 1385–1392.

52 Noginov, M. A.; Zhu, G.; Mayy, M.; Ritzo, B. A.; Noginova, N.; Podolskiy, V. A. Stimulated emission of surface plasmon polaritons. *Phys. Rev. Lett.* **2008**, *101*, No. 226806.

53 Gather, M. C.; Meerholz, K.; Danz, N.; Leosson, K. Net optical gain in a plasmonic waveguide embedded in a fluorescent polymer. *Nat. Photonics* **2010**, *4*, 457–461.